Domain structures in ferromagnetic ultrathin films with in-plane magnetization

J. Castro*
Departamento de Física Aplicada, Universidad de Santiago de Compostela, E-15706 Santiago de Compostela, Spain

S. T. Chui
Bartol Research Institute, University of Delaware, Newark, Delaware 19716

V. N. Ryzhov
Institute for High Pressure Physics, Russian Academy of Sciences, 142 092 Troitsk, Moscow region, Russia
(Received 16 March 1999; revised manuscript received 17 May 1999)

We show that many of the domain patterns in ultrathin films with in-plane magnetizations from experiments and from computer simulations can be well approximated as local extrema of the exchange and anisotropy energies with appropriate boundary conditions. These solutions can be obtained analytically from the many soliton solution of the imaginary time sine-Gordon equation. Different types of these solutions are represented and their physical meaning is discussed. [S0163-1829(99)10537-X]

I. INTRODUCTION

The magnetism of ultrathin films have attracted considerable interest recently.[1,2] This is partly motivated by the possible integration of the semi-conductor microelectronics technology with magnetic elements[1] and possible device applications with the giant magnetoresistive (GMR) and spin tunnelling effect. These systems present opportunities for studying new phenomena that are beginning to be uncovered. The interaction energy between the spins at positions $\mathbf{R},\mathbf{R}'$ is

$$H=0.5\sum_{ij=xyz,\mathbf{RR}'} V_{ij}(\mathbf{R}-\mathbf{R}')S_i(\mathbf{R})S_j(\mathbf{R}'), \qquad (1)$$

where $V=V_d+V_e+V_a$ is the sum of the dipolar energy $V_{dij}(\mathbf{R})=g\nabla_i\nabla_j(1/|\mathbf{R}|)$, the exchange energy $V_e=-J\delta(\mathbf{R}=\mathbf{R}'+d)\delta_{ij}$ between nearest neighbors at distances d, and the crystalline anisotropy energy V_a, g, and J are coupling constants. The form of the anisotropy energy depends on the material of interest. It can be uniaxial (e.g., $V_a=-K\Sigma_i S_{ix}^2$) or fourfold symmetric (e.g., $V_a=-K\Sigma_i[S_{ix}^2-S_{iy}^2]^2/4$), with the easy or hard axis aligned along specific directions.

The magnetic dipoles here can be parallel or perpendicular to the plane.[2–6] For discussions in this paper, we restrict our attention to those cases so that the spins lie in the plane of the film, the case of experimental interest in sensor type applications. The domain pattern depends on the shape of the sample, which is especially important for small structures. In this paper we follow our earlier work[7] and show that the many domain patterns subjected to the sample boundary constraints can be well approximated as local extrema of the exchange and anisotropy energies.

The orientation of the spin is determined by its angle ϕ:

$$\vec{S}=S(\cos\phi,\sin\phi). \qquad (2)$$

For most applications the contribution from the dipolar interaction is small if the global constraint of closed flux lines is satisfied and can be treated as a perturbation. The domain structure is approximately determined by minimizing the exchange and the anisotropy energy which has the form;

$$H=\frac{1}{2}\int d^2r\left[\overline{J}(\phi_x^2+\phi_y^2)+\frac{K}{4}[1-\cos(4\phi)]\right], \qquad (3)$$

and is determined approximately by the equation

$$\nabla^2\phi-0.5K\sin 4\phi/\overline{J}=0, \qquad (4)$$

where both the exchange and a fourfold anisotropy term is incorporated. $\overline{J}\approx zJ/4$ is the effective exchange; z is the number of nearest neighbors and comes from converting the discrete model to the continuum approximation. We shall drop the bar on J in what follows. The exactly soluble sine-Gordon equation[8,9] $(\partial_x^2-\partial_t^2)\phi-0.5K\sin 4\phi/J=0$ is formally the same as the above equation (4) if we transform the y coordinate into the imaginary time it. A simple two-dimensional generalization of the conventional expression for the 90° domain wall has been obtained in our previous work[10] and describes the domain wall that was observed in the experiments on the ultrathin cobalt films.[10,11]

In general, *analytic many soliton* solutions provide for more possibilities to describe the two-dimensional domain wall patterns in thin magnetic films. *Many soliton* solutions are known but have never been exploited in the understanding of domain structures. The main goal of this paper is to represent some exact solutions of the imaginary time sine-Gordon equation which can be used to describe forms of the domain wall patterns in thin magnetic films. We now explain our results in detail.

II. CALCULATION OF THE DOMAIN STRUCTURES

To calculate the domain structures in an ultrathin film with in plane magnetization in the presence of the exchange and an in-plane fourfold anisotropy we have to solve Eq. (4). With the change of variables

$$x' = x\sqrt{\frac{2K}{J}},$$

$$y' = y\sqrt{\frac{2K}{J}}, \tag{5}$$

Eq. (4) becomes

$$-\nabla'^2\phi + \frac{1}{4}\sin 4\phi = 0. \tag{6}$$

In what follows we drop the prime index on the coordinates. In this section we discuss three different ways of obtaining special solutions of this equation in increasing complexity. Some of the results from these different approaches are the same.

A. Waves and solitons

To solve Eq. (6) we first seek trial solutions such that

$$\phi(x,y) = f(\xi) = f(x+uy), \tag{7}$$

where u is a constant. Then

$$(1+u^2)\frac{d^2f}{d\xi^2} = \frac{1}{4}\sin 4f. \tag{8}$$

Then, on integration with respect to f,

$$8(1+u^2)\left(\frac{df}{d\xi}\right)^2 = (C - \cos 4f), \tag{9}$$

where C is an integration constant. Therefore

$$\xi = \int \frac{df}{\pm\sqrt{(C-\cos 4f)/8(1+u^2)}}. \tag{10}$$

We are looking for real solutions; therefore $u^2 \geqslant 0$ and $(df/d\xi)^2 \geqslant 0$. There are various cases depending on the values of C.

Case 1: $C > 1$. $df/d\xi$ has the same sign, positive or negative, for all ξ, and f is a monotonic function of ξ. Equation (10) can be integrated in terms of elliptic functions and gives the periodic solutions of the form

$$f = \frac{\pi}{4} + \frac{1}{2}\sin^{-1}\left\{\pm sn\left(\frac{\xi}{k\sqrt{1+C^2}}, k\right)\right\}, \tag{11}$$

where $k^2 = 2/(C+1)$ and sn is the jacobian elliptic function of modulus k.[12] With respect to ξ the spatial period or wavelength Λ of the periodic function is

$$\Lambda = 4K(k)k\sqrt{1+u^2}, \tag{12}$$

where $K(k)$ represents the complete elliptic integral of the first kind with modulus k.

Case 2: $0 \leqslant C < 1$. In this case we define $f_0 = \frac{1}{4}\cos^{-1}C$, with $0 \leqslant f \leqslant \pi/4$, so that f_0 is the least positive zero of $G(f) = 1 - \cos 4f$. Only when $G(f) \geqslant 0$ are real solutions of f possible. A particular solution is

$$f = \frac{\pi}{4} + \frac{1}{2}\sin^{-1}\left\{\pm\frac{1}{k}sn\left(\frac{\xi}{\sqrt{1+u^2}}, \frac{1}{k}\right)\right\}. \tag{13}$$

This solution represents oscillations of f, such that $f_0 < f < \pi/2 - f_0$ with period $4\sqrt{1+u^2}K(1/k)$. k is related to the parameter C by $k^2 = 2/(C+1)$.

Case 3: $C = 1$. This is a case limit of case 1 and 2 above. Here Eq. (10) gives

$$\xi - \xi_0 = \pm\sqrt{1+u^2}\ln\{\pm\tan f\}, \tag{14}$$

where ξ_0 is a constant and the $\pm$ signs need not be related to one another. Writing this solution in full we have:

$$\phi(x,y) = \pm\tan^{-1}\left\{\pm\sqrt{\frac{2K}{J}}\frac{(x+uy-\xi_0)}{\sqrt{1+u^2}}\right\}. \tag{15}$$

These are the 90° domain wall soliton solutions of Eq. (6). Notice that these solution can also be obtained as a limit of cases 1 and 2 for $k = 1$.

B. Some other explicit solutions

Other simple explicit solutions of Eq. (6) can be obtained as follows. The form of the solution (14) suggest to start from the ansatz suggested by Lamb[13] for the solution of the real time sine-Gordon equation. We seek solutions of Eq. (6) having the form

$$\phi(x,y) = \tan^{-1}[F(x)/G(y)]. \tag{16}$$

Substitution into Eq. (6) gives

$$(F^2+G^2)\left(\frac{F_{xx}}{F} - \frac{G_{yy}}{G}\right) + 2(G_y^2 - F_x^2) - (G^2 - F^2) = 0. \tag{17}$$

Differentiating this equation with respect to x and y we have

$$\frac{1}{(F^2)_x}\left(\frac{F_{xx}}{F}\right)_x = \frac{1}{(G^2)_y}\left(\frac{G_{yy}}{G}\right)_y = A. \tag{18}$$

Integrating these equations we have

$$F_x^2 = \frac{A}{2}F^4 + BF^2 + C,$$

$$G_y^2 = \frac{A}{2}G^4 + (1-B)G^2 + C, \tag{19}$$

for some constants A, B, and C. Equations (19) can be solved generally in terms of elliptic functions, but they have also some special solutions in terms of elementary functions which we first discuss next. This type of solutions is particularly useful for boundary condition considerations, which will be further developed in the next section. Here we consider some special cases when some of the constants A, B, C is zero. We distinguish between the following cases.

Case 1: $A = 0$, $C = 0$, and $0 < B < 1$. This is the soliton solution previously mentioned. The parameter u in Eq. (14) is related to the parameter B by the relationship.

$$u = \pm\sqrt{\frac{1-B}{B}}. \tag{20}$$

Case 2: $A = 0$, $B = C > 0$, we have to distinguish two subclasses. For $B > 1$ we have

$$\phi=\tan^{-1}\left\{\pm\sqrt{\frac{B-1}{B}}\frac{\sinh[\sqrt{2K/J}\sqrt{B}(x-x_0)]}{\sin[\sqrt{2K/J}\sqrt{B-1}(y-y_0)]}\right\} \tag{21}$$

and for $0<B<1$ we have

$$\phi=\tan^{-1}\left\{\pm\sqrt{\frac{1-B}{B}}\frac{\sinh[\sqrt{2K/J}\sqrt{B}(x-x_0)]}{\sinh[\sqrt{2K/J}\sqrt{1-B}(y-y_0)]}\right\}. \tag{22}$$

Equation (21) describes for $B\to 1$, $B>1$ two 90° domain wall separated by a distance of $2\ln(2/\sqrt{B-1})$. As B is increased, the two separated domain walls become separated by vortices and merge into a 180° domain wall. Equation (22) describes a closure domain. This is a case studied by Chui and Ryzhov.[7]

Case 3: $C=0$, $A\neq 0$. F and G depend on A whereas the ratio F/G does not. We have to distinguish three subclasses. For $B>1$ we have

$$\phi=\tan^{-1}\left\{\pm\sqrt{\frac{B}{B-1}}\frac{\sin[\sqrt{2K/J}\sqrt{B-1}(y-y_0)]}{\sinh[\sqrt{2K/J}\sqrt{B}(x-x_0)]}\right\} \tag{23}$$

and for $0<B<1$;

$$\phi=\tan^{-1}\left\{\pm\sqrt{\frac{B}{1-B}}\frac{\sinh[\sqrt{2K/J}\sqrt{1-B}(y-y_0)]}{\sinh[\sqrt{2K/J}\sqrt{B}(x-x_0)]}\right\} \tag{24}$$

and for $B<0$

$$\phi=\tan^{-1}\left\{\pm\sqrt{\frac{|B|}{1+|B|}}\frac{\sinh[\sqrt{2K/J}\sqrt{1+|B|}(y-y_0)]}{\sin[\sqrt{2K/J}\sqrt{|B|}(x-x_0)]}\right\}. \tag{25}$$

Cases 2 and 3 have a simple interpretation. These are two soliton solutions of Eq. (6).

C. Multisoliton solutions

Multisoliton solutions of Eq. (6) can be readily obtained from the Hirota method.[14] We start now with the ansatz

$$\phi=\tan^{-1}\left[\frac{F(x,y)}{G(x,y)}\right] \tag{26}$$

and define the D operator as

$$D_x^m D_y^n(ab)=\left[\left(\frac{\partial}{\partial x}-\frac{\partial}{\partial x'}\right)^m\left(\frac{\partial}{\partial y}-\frac{\partial}{\partial y'}\right)^n \times a(x,y)b(x',y')\right]_{x=x';y=y'}. \tag{27}$$

Equation (6) with the ansatz (26) can be then written as

$$(G^2-F^2)(D_x^2+D_y^2)(FG)-FG(D_x^2+D_y^2)(GG-FF) =FG(G^2-F^2). \tag{28}$$

This can be reduced to two bilinear equations

$$(D_x^2+D_y^2)(FG)=\mu FG, \tag{29}$$

$$(D_x^2+D_y^2)(GG-FF)=(\mu-1)(G^2-F^2),$$

where μ is a constant. We look for solutions of the form

$$G=1+\varepsilon^2 G^{(1)}+\varepsilon^4 G^{(2)}+\cdots,$$

$$F=\varepsilon F^{(1)}+\varepsilon^3 F^{(2)}+\cdots, \tag{30}$$

where ε is a parameter and try to solve Eq. (29) order by order in ε. At zero order we find $G=1$ and $\mu=1$. At first order we have to solve

$$F^{(1)}=F_{xx}^{(1)}+F_{yy}^{(1)}. \tag{31}$$

The simplest nontrivial solution of this equation is

$$F^{(1)}=e^{\vartheta}, \tag{32}$$

where $\vartheta=kx+\omega y+\delta$ and $k^2+\omega^2=1$. For this choice it is possible to make all the other functions zero. Therefore we obtain

$$\phi=\tan^{-1}[\varepsilon e^{kx+\omega y+\delta}]. \tag{33}$$

For $\varepsilon=1$ and $k^2=1/(1+u^2)$ this is the single soliton solution obtained above. To get the two solitons solution we start with a solution of Eq. (31) of the form

$$F^{(1)}=e^{\vartheta_1}+e^{\vartheta_2}, \tag{34}$$

where $\vartheta_i=k_i x+\omega_i y+\delta_i$ and $k_i^2+\omega_i^2=1$. The simplest choice for $G^{(1)}$ which satisfies the equation

$$G_{xx}^{(1)}-F_{xx}^{(1)}F^{(1)}+(F_x^{(1)})^2+G_{yy}^{(1)}-F_{yy}^{(1)}F^{(1)}+(F_y^{(1)})^2=0 \tag{35}$$

is

$$G^{(1)}=A_{(1,2)}e^{\vartheta_1+\vartheta_2} \tag{36}$$

with

$$A_{(1,2)}=\frac{1-k_1k_2-\omega_1\omega_2}{1+k_1k_2+\omega_1\omega_2}=\frac{(k_1-k_2)^2}{(\omega_1+\omega_2)^2}=\frac{(\omega_1-\omega_2)^2}{(k_1+k_2)^2}. \tag{37}$$

Also in this case it is possible to choose all the other functions zero and we obtain for the double soliton solution

$$\phi=\tan^{-1}\left\{\frac{e^{\vartheta_1}+e^{\vartheta_2}}{1+A_{(1,2)}e^{\vartheta_1+\vartheta_2}}\right\}. \tag{38}$$

It is easy to see that solutions (21)–(25) are particular cases of Eq. (38) with an appropriate choice of the constants k_1, k_2, ω_1, ω_2, δ_1, and δ_2. For example, Eq. (22) with the minus sign can be obtained after Eq. (38) with the choices $k_1=-k_2=\sqrt{B}$, $\omega_1=\omega_2=\sqrt{1-B}$, $\delta_1=-\sqrt{B}x_0-\sqrt{1-B}y_0+\ln(\sqrt{(1-B)/B})$, $\delta_2=\sqrt{B}x_0-\sqrt{1-B}y_0+\ln(\sqrt{(1-B)/B})+i\pi$. Some other interesting two-soliton solutions can easily be found after Eq. (38). Making $k_1=k_2=\sqrt{B}$, $\omega_1=-\omega_2=\sqrt{1-B}$, $\delta_1=-\sqrt{B}x_0-\sqrt{1-B}y_0+\ln(\sqrt{B/(1-B)})$, $\delta_2=-\sqrt{B}x_0+\sqrt{1-B}y_0+\ln(\sqrt{B/1-B})+i\pi$, and $\nu=\sqrt{(1-B)/B}$, we obtain

$$\phi=\tan^{-1}(\sinh[\gamma\nu\sqrt{2K/J}(y-y_0)]/\{-\nu\sinh[\gamma\sqrt{2K/J}\times(x-x_0)]\}), \tag{39}$$

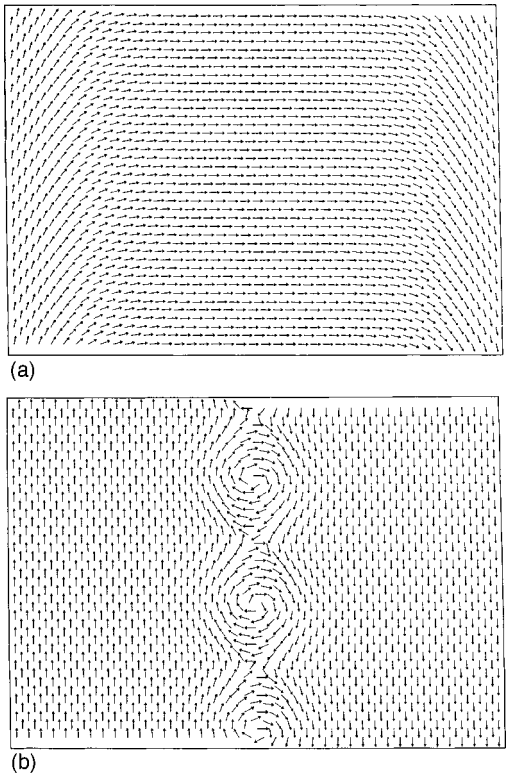

FIG. 1. 180° domain configuration for a rectangle from a two soliton solution [Eq. (41)]. (a) corresponds to $v=0.01$ and (b) to $v=0.8$.

where $\gamma=1/\sqrt{1+v^2}$. The detail of this simple structure has been described previously and will not be repeated here. (See, for example, Fig. 1 of Ref. 7 for the shape of this structure.) Making $k_1=-k_2=\sqrt{1+B}$, $\omega_1=\omega_2=-i\sqrt{B}$, $\delta_1=-\sqrt{1+B}x_0+i\sqrt{B}y_0$, $\delta_2=\sqrt{1+B}x_0+i\sqrt{B}y_0+\ln[\sqrt{B/(1+B)}]+i\pi$, and $v=\sqrt{B/(1+B)}$, we obtain

$$\phi=\tan^{-1}\times\left[\frac{\exp[\gamma\sqrt{2K/J}(x-x_0)]-v^2\exp[-\gamma\sqrt{2K/J}(x-x_0)]}{2\cos[\gamma v\sqrt{2K/J}(y-y_0)]}\right], \tag{40}$$

where $\gamma=1/\sqrt{1-v^2}$. v is related to half the separation of the domain walls x_1' by $v=2e^{-\gamma x_1'}$. In the limit $x_1'\gg 1$ Eq. (40) describes two parallel 90° domain walls located at $x'=x_0'+\ln 2/\gamma$ and $x'=x_0'+\ln 2/\gamma+2x_1'$. Equation (40) takes the most simple form when $e^{-\gamma x_0'}=v$ (Ref. 7):

$$\phi=\tan^{-1}(\cos[\gamma v\sqrt{2K/J}(y-y_0)]/\{v\sinh[\gamma\sqrt{2K/J}\times(x-x_0)]\}). \tag{41}$$

This is basically the same as the solution (21). Figure 1 shows the spin configurations obtained by using Eq. (41) for different values of parameter v for a triangular lattice 40 $\times$40 spins for $J=2$ and $K=0.2$ ($x_0=y_0=0$).

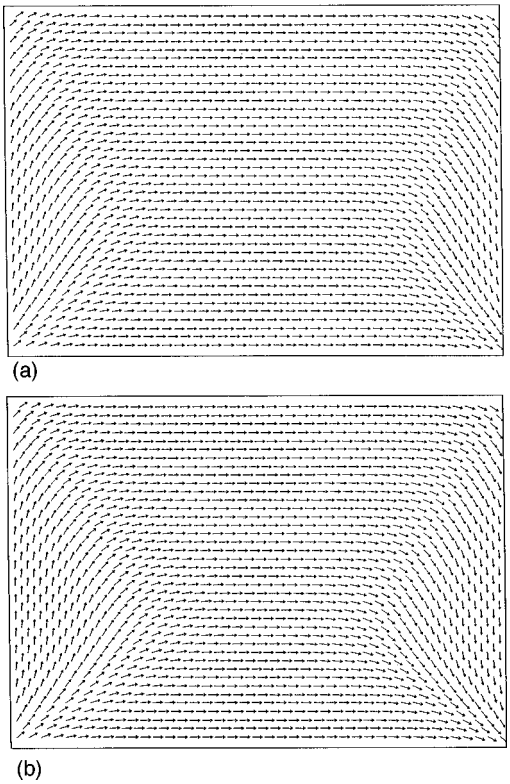

FIG. 2. Edge domain configuration for a rectangle from variational calculations by using Eqs. (41) and (42). (a) represents the case $H=0$ and (b) the case $H=K/2$.

D. Trial solutions to incorporate the dipolar energy

The configurations discussed in this section have so far not taken into consideration the boundary conditions of finite sample boundaries. The magnetostatic energy is lowered if the component of **S** normal to the boundary is equal to zero. This condition can be partially incorporated by using a simple phenomenological generalization of Eq. (41). We suppose that v is a function of y. The form of $v(y)$ is chosen to minimize the magnetostatic energy and is given by

$$v(y)=\frac{A}{\exp[\alpha\sqrt{2K/J}(y+y_0)]+\exp[-\beta\sqrt{2K/J}(y+y_0)]}, \tag{42}$$

where $\alpha=\ln(A/v_0)/(L_y/2+y_0)$, $\beta=\ln(A/v_0)/(L_y/2-y_0)$, $v_0=2\exp(-\sqrt{2K/J}L_x/2)$, and L_x and L_y are the sample sizes in x and y directions, respectively. The parameters A and y_0 are obtained by minimizing the total energy of the system. In Fig. 2 the spin configurations obtained by using Eqs. (41) and (42) are shown for a triangular lattice 40$\times$40 spins for $J=2$, $K=0.2$, and $g=1$. Figure 2(a) corresponds to magnetic field $H=0$ and Fig. 2(b) to $H=K/2$. This can be compared with the Monte Carlo result discussed in the next section and shown in Fig. 7. The total energy per particle is $E_t=-8.39387$ for $H=0$ and $E_t=-8.31041$ for $H=K/2$. The parameters A and y_0 are $A=0.027373$, $y_0=7.4435$ for $H=0$ and $A=0.084793$, $y_0=6.6731$ for $H=K/2$. Equations (41) and (42) may be used to investigate the behavior of the spin system under different system parameters. However,

Eq. (42) cannot be obtained as the exact solution of the Eq. (4) for the finite sample. Exact solutions for this case are discussed in the next section.

E. *N* soliton solution

For completeness we end this section by considering the *N*-solitons solution of Eq. (6). We take as solution of Eq. (31):

$$F^{(1)}=\sum_i e^{\vartheta_i}, \tag{43}$$

where $\vartheta_i=k_i x+\omega_i y+\delta_i$ and $k_i^2+\omega_i^2=1$. The simplest choice for $G^{(1)}$ is

$$G^{(1)}=\sum_{i<j} A_{(i,j)}e^{\vartheta_i+\vartheta_j}, \tag{44}$$

with

$$A_{(ij)}=\frac{1-k_ik_j-\omega_i\omega_j}{1+k_ik_j+\omega_i\omega_j}=\frac{(k_i-k_j)^2}{(\omega_i+\omega_j)^2}=\frac{(\omega_i-\omega_j)^2}{(k_i+k_j)^2}. \tag{45}$$

Also in this case is possible to choose all the other functions zero and we obtain for the *N* solitonic solution

$$\phi=\tan^{-1}\left\{\frac{\Sigma_i e^{\vartheta_i}}{1+\Sigma_{i<j}A_{(i,j)}e^{\vartheta_i+\vartheta_j}}\right\}. \tag{46}$$

III. BOUNDARY CONDITIONS

The consideration of domain patterns in small structures requires the imposition of finite boundary conditions. There are different possible ways to determine the parameters. One possibility is to require the surface part of the magnetostatic energy to be equal to zero. This imposes the boundary conditions that the normal components of the magnetization must be zero at the boundary of the rectangle. We first discuss examples of this for different cases. In the case of periodic solutions, Eq. (11), finite boundary conditions only impose conditions in the k values. For example for $c=0$ the solution depends only on x and $f(0)=f(L)=\pm\pi/2$ we have

$$f=\pm\frac{\pi}{2}+\frac{1}{2}\sin^{-1}\left\{\pm sn\left(\frac{x}{k_n},k_n\right)\right\}, \tag{47}$$

where k_n is related to the sample size L by the equation

$$2nK(k_n)=\frac{L}{k_n}. \tag{48}$$

This solution corresponds to a spin density wave of period

$$\Lambda=4k_nK(k_n). \tag{49}$$

Another important type of solutions can be obtained starting from the ansatz of Eq. (16), with the solutions to Eq. (19) in terms of Jacobian elliptic functions with the appropriate boundary conditions.[15] As an example we consider configurations corresponding to edge domains with the boundary conditions of that the spins point down (up) on the left (right) edges and horizontally in both the top and bottom edge. This is equivalent to imposing the boundary conditions

$$F\left(\frac{\pm L_x}{2}\right)\to\pm\infty,$$

$$G^{-1}\left(\frac{\pm L_y}{2}\right)=0, \tag{50}$$

where L_x and L_y are the sample sizes in the x and y directions, respectively. One class of solutions for which these boundary conditions can be easily imposed is

$$\phi=\tan^{-1}\{Dtn[\Omega(x-x_0),\lambda_f]cn[v(y-y_0),\lambda_g]\}, \tag{51}$$

where

$$\lambda_f^2=\frac{D^2+\Omega^2(1-D^2)^2}{\Omega^2(1-D^2)},$$

$$\lambda_g^2=-\frac{D^2\Omega^2(1-D^2)}{\Omega^2(1-D^2)^2-1},$$

$$v^2=\frac{\Omega^2(1-D^2)^2-1}{1-D^2}. \tag{52}$$

For a rectangular sample, the boundary condition can be incorporated by demanding that *tn* to be infinite at the two vertical boundaries $x=-a=-L_x/2$ and $x=a$ and *cn* to be zero at the horizontal boundaries $y=-b=-L_x/2$ and $y=b$. We first consider solutions of this type for different parameter values. We consider the case $D^2<1$ because the opposite case leads to the same results. We describe different regimes in the parameter space for D and Ω. In some cases, the right hand sides of Eqs. (52) becomes less than zero. Some of the parameters λ_f, λ_g, and v may become imaginary. It is then necessary to rewrite the elliptic functions with imaginary arguments in terms of functions of real arguments. Let us consider now these different forms of the solution (51) in detail.

A. $\Omega^2>1/(1-D^2)^2$

From Eq. (52) $\lambda_f^2>0$, $v^2>0$, $\lambda_g^2<0$, the solution has the form

$$\phi=\tan^{-1}\left[Dtn[\Omega(x-x_0),\lambda_f]\frac{cn[v\sqrt{1+k_g^2}(y-y_0),k_{1g}]}{dn[v\sqrt{1+k_g^2}(y-y_0),k_{1g}]}\right], \tag{53}$$

where $k_g^2=-\lambda_g^2$ and $k_{1g}^2=k_g^2/(1+k_g^2)=D^2\Omega^2(1-D^2)/[\Omega^2(1-D^2)-1]$. These solutions represent edge domains which shall be discussed in more detail below. For $\Omega^2\to1/(1-D^2)^2$ the solution (53) becomes

$$\phi=\tan^{-1}\{Dtn[(x-x_0)/(1-D^2),1-D^4]\}. \tag{54}$$

This limit corresponds to two straight domain walls that are far apart.

B. $1/(1-D^2)<\Omega^2<1/(1-D^2)^2$

We have $\lambda_f^2>0$, $\lambda_g^2>0$, $v^2<0$; the solution takes the form

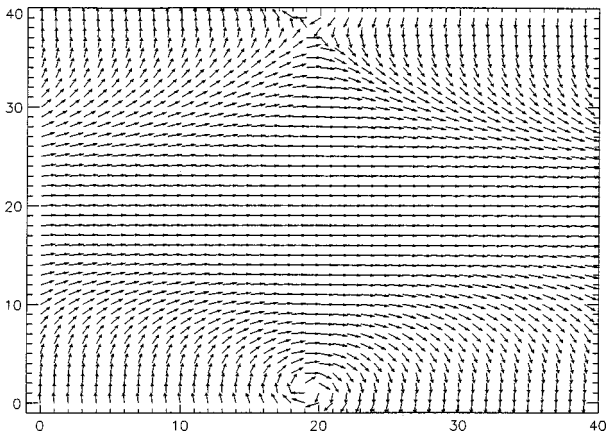

FIG. 3. Two-dimensional spin configuration obtained after Eq. (57); see text.

$$\phi=\tan^{-1}\left[Dtn[\Omega(x-x_0),\lambda_f^2]\frac{dn[\omega\lambda_g(y-y_0),\lambda_{1g}]}{cn[\omega\lambda_g(y-y_0),\lambda_{1g}]}\right], \tag{55}$$

where $\omega^2=-\nu^2$ and $\lambda_{1g}^2=[\Omega^2(1-D^2)-1]/[D^2\Omega^2(1-D^2)]$. The limiting behavior of Eq. (55) coincides with Eq. (54) for $\Omega^2\to 1/(1-D^2)^2$. For $\Omega^2=1/(1-D^2)$ it has the form

$$\phi=\pi/2-\tan^{-1}\left[\frac{\cos[D/\sqrt{1-D^2}(y-y_0)]}{D\sinh[(x-x_0)/\sqrt{1-D^2}]}\right]. \tag{56}$$

Equation (56) coincides with the two domain wall solution (41) with D playing the role of the parameter ν.

C. $\Omega^2<1/(1-D^2)$

We have $\lambda_f^2>1$, $\lambda_g^2>0$, $\nu^2=-\omega^2<0$. Expression (51) may be rewritten in the form;

$$\phi=\tan^{-1}\left[\frac{D}{\lambda_f}\frac{sn[\lambda_f\Omega(x-x_0),1/\lambda_f]}{dn[\lambda_f\Omega(x-x_0),1/\lambda_f]}\frac{1}{cn[\omega(y-y_0),\lambda_g']}\right], \tag{57}$$

where $\lambda_g'^2=1-\lambda_g^2=[1-\Omega^2(1-D^2)]/[1-\Omega^2(1-D^2)^2]$. An example of this configuration is shown in Fig. 3 for $D=0.125$, $\Omega=0.1$, $J=2$, $K=0.2$. The limiting behavior of Eq. (57) for $\Omega^2\to 1/(1-D^2)$ coincides with Eq. (56). By using the relation $cn(u-K,k)=\sqrt{1-k^2}sn(u,k)/dn(u,k)$ Eq. (57) can be rewritten as

$$\phi=\tan^{-1}\left[\frac{D}{\lambda_f\lambda_g}\frac{sn[\lambda_f\Omega(x-x_0),1/\lambda_f]}{dn[\lambda_f\Omega(x-x_0),1/\lambda_f]}\frac{dn[\omega(y-y_0),\lambda_g']}{sn[\omega(y-y_0),\lambda_g']}\right]. \tag{58}$$

In the limit $\Omega^2\to 1/(1-D^2)$ the solution takes the form

$$\phi=\pi/2-\tan^{-1}\left[\frac{\sin[D/\sqrt{1-D^2}(y-y_0)]}{D\sinh[(x-x_0)/\sqrt{1-D^2}]}\right]. \tag{59}$$

Equation (59) can be obtained from Eq. (56) by shift in the y coordinates. In the limit of Ω approaching zero but finite D, an equivalent limit is obtained. When $\Omega^2<1$ the limit $D\to 0$ yields an expression

$$\phi=\pi/2-\tan^{-1}\left[\frac{\Omega}{\sqrt{1-\Omega^2}}\frac{\sinh[\sqrt{1-\Omega^2}(y-y_0)]}{\Omega\sinh(x-x_0)}\right], \tag{60}$$

which is reduced to the closure domain Eq. (39) after the substitution $\sqrt{1-\Omega^2}/\Omega=\nu$. The closure domain configurations may also be obtained from Eqs. (53), (55), and (57) by using a shift in y coordinates by one quarter of the period of elliptic functions $K(k)$ where $K(k)$ is the complete elliptic integral of the first kind. In the limit of small Ω, $D/\lambda_F\to\Omega\sqrt{1-D^2}$, $\lambda_f\Omega\to D/\sqrt{1-D^2}$, $\omega\to 1/\sqrt{1-D^2}$, $\lambda_g'\to 1$

$$\phi\to\tan^{-1}\left[\frac{1}{\Omega\gamma}\frac{\sin[D\gamma(x-x_0)]}{\mathrm{sech}[\gamma(y-y_0)]}\right],$$

where $\gamma=1/\sqrt{1-D^2}$.

We now return to a general discussion of the domain configurations. Another interesting solution would be to consider configurations corresponding to edge domains with the boundary condition of that the spins point up (up) on the left (right) edges and horizontally in both the top and bottom edge. This is equivalent to impose the boundary conditions

$$F\left(\frac{\pm L_x}{2}\right)\to\infty,$$

$$G^{-1}\left(\frac{\pm L_y}{2}\right)=0, \tag{61}$$

where L_x and L_y are the sample sizes in the x and y directions, respectively. The solution we are looking for have the form

$$\phi=\tan^{1}\left[D\frac{ds[\Omega(x-x_0),\lambda_f]}{nc[\nu(y-y_0),\lambda_g]}\right]. \tag{62}$$

This corresponds to a solution of the Eq. (19) if we have

$$\Omega^2=\nu^2D^2(1-\lambda_g^2),$$

$$D^2\Omega^2(1-\lambda_f^2)\lambda_f^2=\nu^2\lambda_g^2,$$

$$\Omega^2(2\lambda_f^2-1)=1-\nu^2(2\lambda_g^2-1). \tag{63}$$

Imposing the boundary conditions we have $x_0=y_0=0$ and

$$\Omega\frac{L_x}{2}=K(\lambda_f),$$

$$\nu\frac{L_y}{2}=K(\lambda_g). \tag{64}$$

Inserting this into the above equation we have

$$\left(\frac{2K(\lambda_f)}{L_x}\right)^2=\left(\frac{2K(\lambda_g)}{L_y}\right)^2D^2(1-\lambda_g^2),$$

$$\left(\frac{2K(\lambda_f)}{L_x}\right)^2(2\lambda_f^2-1)=1-\left(\frac{2K(\lambda_g)}{L_y}\right)^2(2\lambda_g^2-1),$$

$$D^2\left(\frac{2K(\lambda_f)}{L_x}\right)^2(1-\lambda_f^2)\lambda_f^2=\lambda_g^2\left(\frac{2K(\lambda_g)}{L_y}\right)^2. \tag{65}$$

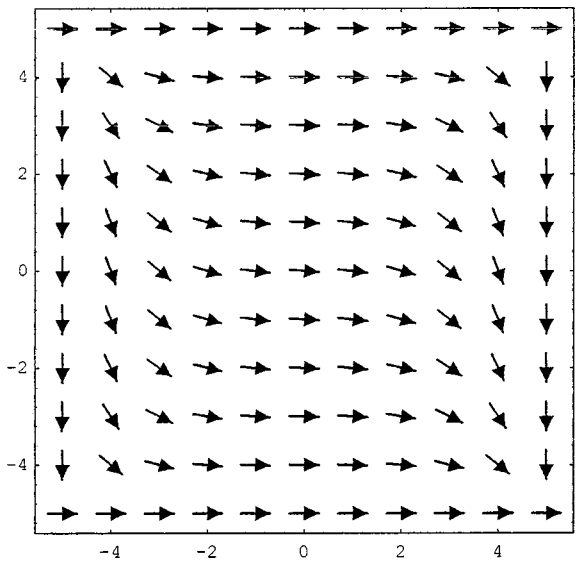

FIG. 4. Two-dimensional spin configuration obtained after Eq. (62); see text.

This system of equations must be solved numerically to obtain λ_g, λ_f, and α. Then on substitution in equations (64) we can calculate k and Ω and this completes our calculus of the solution of Eq. (6) with the given boundary conditions. This solution for the case $L_x=L_y=10$ is represented in Fig. 4.

We can extend our solutions (22) for the closure domains to the case of a finite sample. The solutions we are looking for have the form

$$\phi=\tan^{-1}\left[D\,\frac{sc[\Omega(x-x_0),\lambda_f]}{sc[\nu(y-y_0),\lambda_g]}\right]. \tag{66}$$

This corresponds to a solution of Eq. (19) if we have

$$\Omega^2(1-\lambda_f^2)=\nu^2\alpha^2(1-\lambda_g^2),$$

$$D^2\Omega^2=\nu^2,$$

$$\Omega^2(2-\lambda_f^2)=1-\nu^2(2-\lambda_g^2). \tag{67}$$

To impose the boundary conditions we assume that we are dealing with a square lattice with $1\leqslant L_x\leqslant 2N_x$, $1\leqslant L_y\leqslant 2N_y$ and the defect is centered at $(x_0,y_0)=(N_x+\frac{1}{2},N_y+\frac{1}{2})$. Then we have

$$\Omega(N_x-\tfrac{1}{2})=K(\lambda_f),$$

$$\nu(N_y-\tfrac{1}{2})=K(\lambda_g). \tag{68}$$

Inserting this into the above equation we have

$$\left(\frac{K(\lambda_f)}{2N_x-1}\right)^2(1-\lambda_f^2)=\left(\frac{K(\lambda_g)}{2N_y-1}\right)^2D^2(1-\lambda_g^2),$$

$$\left(\frac{2K(\lambda_f)}{2N_x-1}\right)^2(2-\lambda_f^2)=1-\left(\frac{2K(\lambda_g)}{2N_y-1}\right)^2(2-\lambda_g^2),$$

$$D^2\left(\frac{K(\lambda_f)}{2N_x-1}\right)^2=\left(\frac{K(\lambda_g)}{2N_y-1}\right)^2. \tag{69}$$

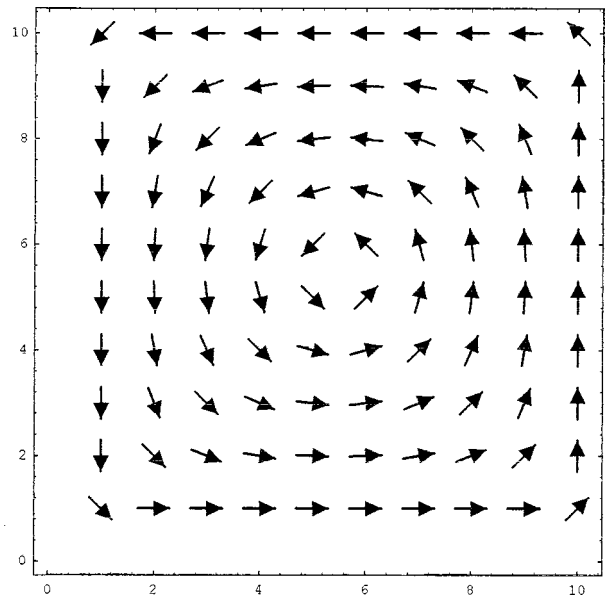

FIG. 5. Two-dimensional spin configuration obtained after Eq. (66); see text.

This system of equations must be solved numerically to obtain λ_g, λ_f, and D. Then on substitution in Eq. (68) we can calculate ν and Ω and this completes our calculus of the solution of Eq. (6) with the given boundary conditions. This solution for the case $L_x=L_y=10$ is represented in Fig. 5. A simple approximation of the closure domain solution, Eq. (60) can be obtained in terms of elementary functions for a square lattice of dimensions $L_x=L_y>10$. For $L_x=L_y$ we expect by symmetry considerations that $\lambda_f=\lambda_g$ and $\Omega=\nu$. Then we have $D=\pm 1$. Furthermore for $L_x=L_y>10$ we can approximate $\lambda_f=\lambda_g\approx 1$. Therefore $\nu=\Omega=1/\sqrt{2}$. We have obtained a simple approximation to Eq. (61)

$$\phi=\arctan\left\{\pm\frac{\sinh 1/\sqrt{2}(x-x_0)}{\sinh 1/\sqrt{2}(y-y_0)}\right\}. \tag{70}$$

This corresponds to Eq. (22) with $B=\frac{1}{2}$. We have compared the approximate solution with the exact one for a $L_x=L_y=10$ square lattice and we have found a value of the mean square difference between the azimuthal angles in both solutions of about 0.08 rad.

D. Edge domains in detail

Quite often good analytic approximations exists for the solutions of the boundary conditions. We discuss in detail an example of this for the calculation of the parameters of the edge domains in Eq. (53). As mentioned above, in this case $tn[\Omega(x-x_0)]$ must be infinite at the vertical boundaries and $cn[\nu\sqrt{1+k_g^2}(y-y_0),k_{1g}]$ must be zero at the horizontal boundaries. Therefore $x_0=y_0=0$ and

$$\Omega\sqrt{2K/J}a=K(\lambda_f),$$

$$\nu\sqrt{1+k_g^2}\sqrt{2K/J}b=K(k_{1g}). \tag{71}$$

For large enough values of the half horizontal and vertical box sizes a and b $\lambda_f\to 1$, $k_{1g}\to 0$ and Eqs. (71) can be approximated by

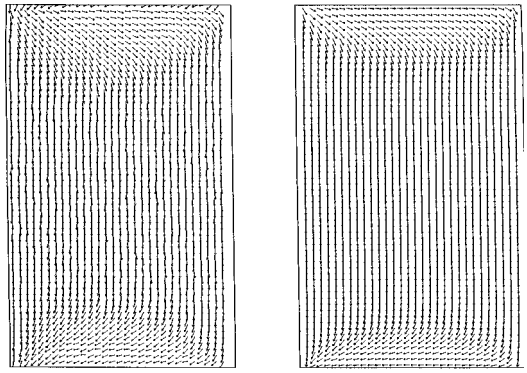

FIG. 6. Edge domain configuration for a rectangle from a two soliton solution. The analytic results are in (b). The finite temperature Monte Carlo results observed in Ref. 10 are shown in (a).

$$\Omega\sqrt{2K/J}a=0.5\ln[16/(1-\lambda_f^2)],$$

$$v\sqrt{1+k_g^2}\sqrt{2K/J}b=\pi/2. \tag{72}$$

From the definition of k_g and v, we get $v\sqrt{1+k_g^2}\approx\sqrt{\Omega^2-1}$. These equations have the simple approximate solution:

$$\Omega\approx\sqrt{1+(\pi/2b')^2},$$

$$D\approx 4\Omega e^{-\Omega a'}/\sqrt{\Omega^2-1}. \tag{73}$$

Here $a'=\sqrt{2K/J}a$ and $b'=\sqrt{2K/J}b$. The second equation of Eq. (73) is obtained directly from the second of Eq. (72). We have also solved the boundary conditions numerically with the bisection algorithm for solving nonlinear equations. The difference between the numerical and approximate results is less than 0.01% for Ω and less than 3% for D. Using the approximation $tn(u,\lambda_f)\approx\sinh(u)$ for $\lambda_f\approx 1$ and $cn(u,k)\approx\cos(u)$, $dn(u,k)\approx 1$ for $k\approx 0$, we obtain $\phi\approx\tan^{-1}[8b'\exp(-a')\sinh(x)\cos(\pi y/2b)/\pi]$, where w is given by $w^{-1}=\sqrt{2K/J}+\pi^2/(8b^2)\sqrt{J/2K}$. For the sake of completeness, we show in Fig. 6(a) the edge domain pattern obtained by using Eqs. (53) and (73) for the system of 40 $\times$40 particles ($J=2$, $K=0.1J$, $g=0.5J$, $J=-1.5J$, and the lattice constant $a_0=1$). Figure 6(b) shows the results of the Monte Carlo simulation for this system in zero magnetic field. There are other metastable solutions where the period in the y direction is smaller. This corresponds to replacing the factor $\cos(\pi y/2b)$ by $\cos[\pi(2n+1)y/2b]$. These type of solutions exhibit more singularities at the edges and is often observed experimentally as well as in simulations. An example of this is shown in Fig. 7 for $n=1$ ($J=2$, $K=0.1333$ $g=0.5$ for a square lattice of 60$\times$60 spins). More generally one can consider D and Ω in Eq. (51) as the variational parameters which can be determined by minimizing the total energy of the system. For the same parameters as that at the end of Sec. II at zero field minimization of the energy gives $\Omega=1.024$, $D=0.006$, and the energy per particle $E_{\min}=-8.39035$. This energy is close to that (-8.39387) obtained by using the variational approach at the end of Sec. II. From the boundary condition constraint [Eqs. (73)] we have $\Omega=1.032$, $D=0.01$, and the energy corresponding to these parameters is $E_b\approx-8.371$. Therefore the simple equations (53) and (73) may be considered as the reliable starting point for the quantitative investigation of the edge domain patterns. Minimizing the energy of the closure domain configuration described by the Eq. (60) we have $D_v\approx 0$, $\Omega_v=0.632$, $E_{\min}=-8.49$. This result exactly coincide with the minimum of the total energy obtained by using Eq. (39) to describe the closure domain configuration. This minimum corresponds to $v=1.23=\sqrt{1-\Omega_v^2}/\Omega_v$. So the simple formula (39) obtained for the infinite sample may be used to describe closure domain patterns for finite size systems provided the system size is not extremely small.

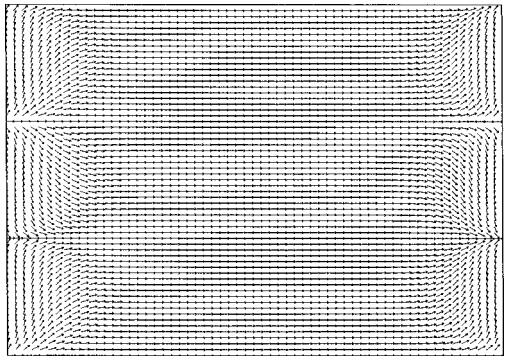

FIG. 7. Edge domain configuration of zero vorticity with more edge singularities.

E. Vorticity

The edge domain in case 1 corresponds to configurations of ''finite vorticity'' wherein the magnetizations along the two vertical edges are opposite to each other. Let us consider now the exact two soliton solution of Eq. (4) corresponding the configuration with parallel edge domain magnetization. Keeping in mind that the spins point down at the left and right edges of the rectangle and horizontally at both the top and bottom edges we find

$$\phi=\tan^{-1}\{Dcn[i\Omega(x-x_0),\lambda_f]cn[v(y-y_0),\lambda_g]\}$$

$$=\tan^{-1}\left[\frac{D}{cn[\Omega(x-x_0),k']}cn[v(y-y_0),\lambda_g]\right], \tag{74}$$

where $k'=\sqrt{1-\lambda_f^2}$ and

$$\lambda_f^2=\frac{D^2[\Omega^2(1+D^2)-1]}{\Omega^2(1+D^2)^2},$$

$$\lambda_g^2=\frac{D^2(\Omega^2+D^2\Omega^2+D^2)}{(1+D^2)[\Omega^2(1+D^2)+D^2-1]},$$

$$v^2=\frac{D^2\Omega^2+\Omega^2+D^2-1}{1+D^2},$$

$$k'^2=1-\lambda_f^2=\frac{\Omega^2+\Omega^2D^2+D^2}{\Omega^2(1+D^2)^2}. \tag{75}$$

Physically interesting results can be obtained for $\Omega^2\geqslant 1/(1+D^2)$. In this case $\lambda_f^2\geqslant 0$, $v^2\geqslant 0$, $k'^2\leqslant 1$, $\lambda_g^2\leqslant 1$. First consider the limiting behavior of the solution for $\Omega^2=1/(1$

$+D^2$). One has $k'^2=\lambda_g^2=1$, $v^2=D^2/(1+D^2)$. Taking into account that $cn(u,1)=\mathrm{sech}(u)$, we find

$$\phi(x,y)=\tan^{-1}\left[\frac{Dch[(x-x_0)/\sqrt{1+D^2}]}{ch[D(y-y_0)/\sqrt{1+D^2}]}\right]. \tag{76}$$

To determine the parameters D and Ω in Eq. (74), we assume that the normal component of magnetization is zero at the boundary of the rectangle. In this case $x_0=y_0=0$ and the boundary conditions have the form

$$\Omega x|_{x=\pm a'}=K(k'),$$

$$vy|_{y=\pm b'}=K(\lambda_g). \tag{77}$$

We assume $D^2\ll 1$ so that $k'\approx 1$ and $\lambda_g\ll 1$. In this case $K(\lambda_g)\approx\pi/2$, $K(k')\approx\ln(4/\lambda_f)=0.5\ln(16/\lambda_f^2)$, and the approximate solution of the equations for Ω and D coincides with Eqs. (73). Taking into account that $v\approx\pi/(2b')$, and for $\lambda_g\ll 1$ the elliptic function $cn(vy,\lambda_g)\approx\cos[(\pi y)/(2b')]$, we find the final expression

$$\phi(x,y)\approx\tan^{-1}\left[\frac{4\Omega}{\sqrt{\Omega^2-1}}e^{-a'\Omega}ch(\Omega x)\cos\left(\frac{\pi}{2}\frac{y}{b'}\right)\right]$$

$$\approx\tan^{-1}\left[\frac{8b'}{\pi}e^{-a'}ch(x)\cos\left(\frac{\pi}{2}\frac{y}{b'}\right)\right]. \tag{78}$$

An example of such zero vorticity edge domains is shown in Fig. 7.

IV. CONCLUSION

In this paper we have provided details about different 2 soliton solutions of the imaginary time sine Gordon equation and their application and interpretation of different domain structures. The effect of dipolar interaction is taken as a boundary constraint here but is otherwise not included. The residual effect of the dipolar interaction is usually slight and has been discussed recently, with particular emphasize to multilayer structures.[16]

ACKNOWLEDGMENTS

This work was supported in part by the Office of Naval Research under Contract No. N00014-94-1-0213. V.N.R. acknowledges the financial support from the Russian Science Foundation through the Grant No. 98-02-16805 and the hospitality of the Bartol Research Institute. Many valuable discussions with Dr. J. W. Tucker are gratefully acknowledged.

*Electronic address: facastro@usc.es

[1] G. Prinz, Science **1092**, 250 (1990).
[2] B. Heinrich and J. F. Cochran, Adv. Phys. **42**, 524 (1994).
[3] S. T. Chui, Phys. Rev. Lett. **74**, 3896 (1995).
[4] S. T. Chui, Phys. Rev. B **50**, 12 599 (1994).
[5] A. Berger and H. P. Oepen, Phys. Rev. B **45**, 12 596 (1992).
[6] A. Berger and H. P. Oepen, J. Magn. Magn. Mater. **121**, 102 (1993).
[7] S. T. Chui and V. N. Ryzhov, Phys. Rev. Lett. **78**, 2224 (1997).
[8] G. Eilenberger, *Solitons. Mathematical Methods for Physicists* (Springer-Verlag, New York, 1981).
[9] V. E. Zakharov, S. V. Manakov, S. P. Novikov, and L. P. Pitaevsky, *Theory of Solitons* (Consultants Bureau, New York, 1984).
[10] S. T. Chui and V. N. Ryzhov, J. Magn. Magn. Mater. **182**, 25 (1998).
[11] H. P. Oepen, J. Magn. Magn. Mater. **93**, 116 (1991).
[12] H. Jeffreys and B. Jeffreys, *Methods in Mathematical Physics* (Cambridge University Press, Cambridge 1992).
[13] G. L. Lamb, Jr., Rev. Mod. Phys. **43**, 99 (1971).
[14] R. Hirota, Prog. Theor. Phys. **52**, 1498 (1974).
[15] P. F. Byrd and M. D. Friedman, *Handbook of Elliptic Integrals for Engineers and Physicists* (Springer-Verlag, Berlin, 1954).
[16] S. T. Chui and V. N. Ryzhov, J. Magn. Magn. Mater. **177**, 1303 (1998).